

Supplement of Atmos. Chem. Phys., 16, 13015–13034, 2016  
<http://www.atmos-chem-phys.net/16/13015/2016/>  
doi:10.5194/acp-16-13015-2016-supplement  
© Author(s) 2016. CC Attribution 3.0 License.



Atmospheric  
Chemistry  
and Physics  
Open Access  
EGU

*Supplement of*

## **Seasonal variation of tropospheric bromine monoxide over the Rann of Kutch salt marsh seen from space**

**Christoph Hörmann et al.**

*Correspondence to:* Christoph Hörmann (c.hoermann@mpic.de)

The copyright of individual parts of the supplement might differ from the CC-BY 3.0 licence.

## S1 Industrial salt evaporation complexes in the Rann of Kutch

Large industrial evaporation ponds are located near the coast of the *Great and Little Rann of Kutch* (see also Figure 2a, left in the main paper) and are used for the production of salt and the subsequent recovery of elemental bromine from sea bittern. Especially all over the *Little Rann*, the salt is also harvested from hand-built salt evaporation ponds that are constructed by thousands of local families year after year, after having been destroyed by the annually recurring monsoon flood.

A significant contribution of halogen emissions from the large artificial evaporation ponds that are used for salt/bromine mining can, however, be ruled out, as no trend can be seen from the measurements although the industrial facilities were massively expanded after 2009. Figure S1 shows MODIS Band 7-2-1 images for the *Rann of Kutch* area in January 2005 and December 2014. The artificial evaporation ponds, marked by red circles, can be identified by water that appears in dark blue in contrast to the bright salty surface that appears light blue. A direct comparison of both panels clearly shows that the number and extent of the industrial salt mining complexes increased strongly during the time frame of the analyzed OMI data set. Most of the additional facilities that show up in Figure S1 (right) were built in 2009/2010. A closer look to such evaporation ponds is given in Figs. S2 and S3, where Landsat images from Google Earth<sup>®</sup> are shown for the regions indicated by **a** and **b** in Figure S1 (right).

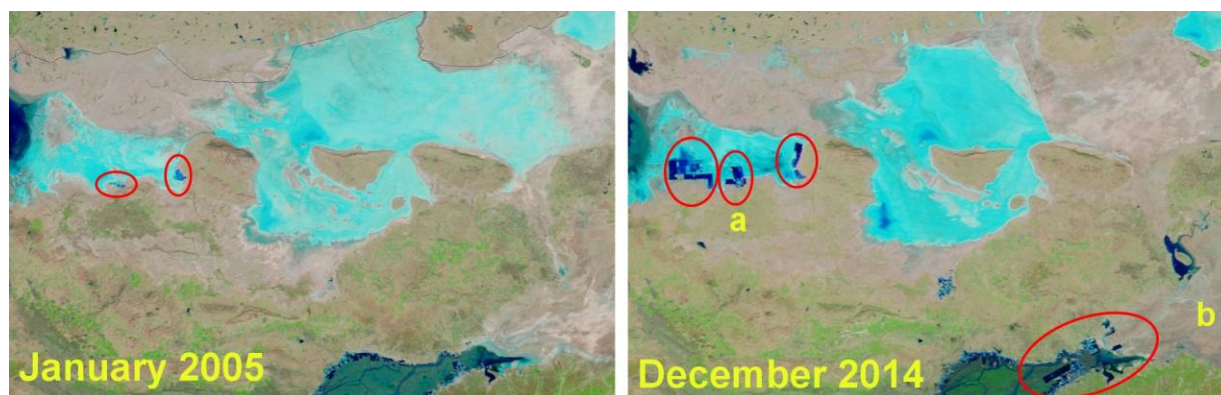


**Figure S1.** MODIS Band 7-2-1 observations over the Rann of Kutch area in January 2005 (left) and December (2014), indicating the massive extension of industrial salt mining complexes that can be identified by water inside the evaporation ponds appearing in dark blue (additionally marked by red circles). Landsat images from Google Earth<sup>®</sup> for regions **a** and **b** can be found in Figs. S2 and S3.



**Figure S2.** Landsat images from Google Earth® indicating the large industrial salt/bromine mining complexes including evaporation ponds at the western part of the Great Rann of Kutch. The right panel shows a zoomed version of the facility that is marked by the yellow rectangle of the left panel. The major part of the evaporation ponds were built in 2009/2010.



**Figure S3.** Landsat images from Google Earth® indicating hand-built salt evaporation ponds all over the Little Rann of Kutch that are constructed by thousands of local families year after year. The right panel shows a zoomed version of the facility that is marked by the yellow rectangle of the left panel. All evaporation ponds are rebuilt after having been destroyed by the annually recurring monsoon flood.

## S2 Distribution of BrO compared to high reflectivity

The contrast between the Rann and the surroundings changes during the year, not only because of the varying absolute albedo of the salt marsh, but also because of that in the surrounding region. It is therefore very important to make sure that the "differential albedo" doesn't affect the polynomial stratospheric background correction and in a worst case scenario might lead to a spurious enhancement/decrement of the final retrieved BrO VCDs over the Rann. To minimize this risk, an extensive area surrounding the Rann is used for the stratospheric background correction (18-30°N and 62-78°E; this essentially encompasses the whole area shown in the monthly BrO maps in Figure 3 of the manuscript). The actual Rann area (22.5-25.5°N and 67.5-72.5°E) was completely excluded from the 2D polynomial fit to make sure that the differential albedo between the Rann and the surrounding area doesn't affect this approach (Section 3.2 of the manuscript).

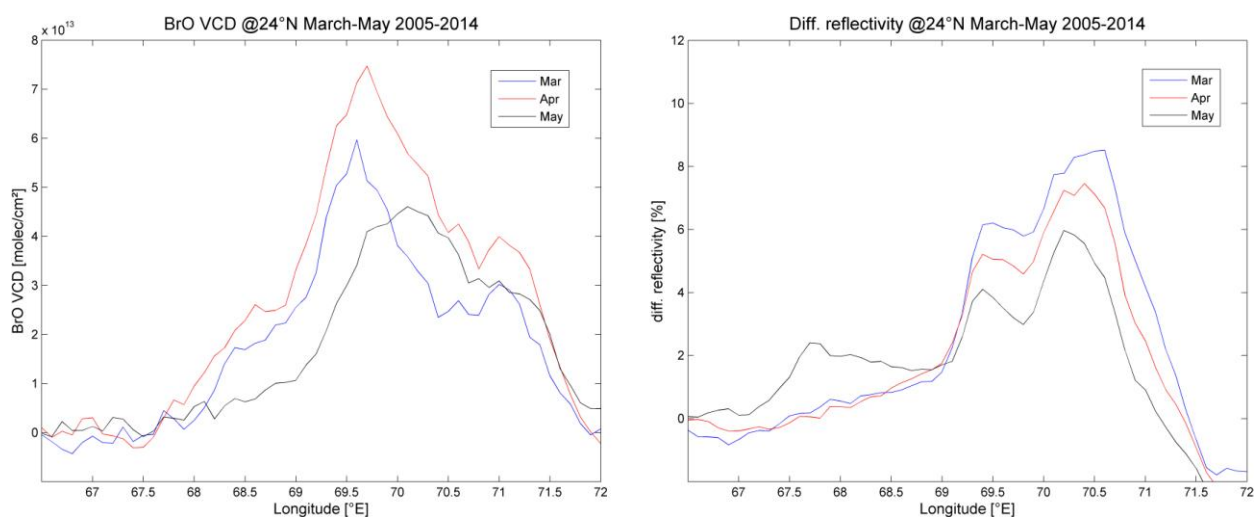


**Figure S4.** Mean BrO VCD (left) and differential reflectivity (right) in longitudinal direction over the Great Rann of Kutch at 24°N latitude for March-May 2005–2014 (color coded in blue - March, red - April and black - May).

In the following, the reflectivity of the Rann region was normalized by the mean reflectivity in a nearby area (the reference area mentioned in Section 4.2 of the manuscript: 22.5-25.5°N/62-67°E) for all months during the time period 2005–2014 to further investigate a possible correlation between enhanced surface albedo and the BrO VCDs. Figure S4 (right) shows the normalized reflectivity in longitudinal direction over the Great Rann (24°N latitude) along with the increasing BrO VCDs (left) during March-May 2005-2014 (color coded in blue - March, red - April and black - May), illustrating the change of contrast between Rann and surrounding areas. While the BrO VCDs are already enhanced during March, peak in April and clearly decrease and shift towards East in May, it is obvious from the normalized reflectivity that there is a continuous decrease of the Rann albedo at the same time (please note that the enhanced reflectivity at 67.5°E during May results from increasing cloud coverage at the western coast in the run-up to the monsoon season).

During winter time (December–February), the differential reflectivity over the Rann (and therefore the contrast between the

Indian Ocean and the salt marsh) is even higher, but shows only little variation (Figure S4, right). The corresponding BrO VCDs are only slightly enhanced and also show very low variation, although the upcoming increase seems to already start slowly in February (Figure S4, left). It is important to note that the spatial patterns of the reflectivity and the BrO VCDs are quite different, indicating that the observed enhanced tropospheric BrO VCDs are not a possible artifact caused by the albedo contrast.

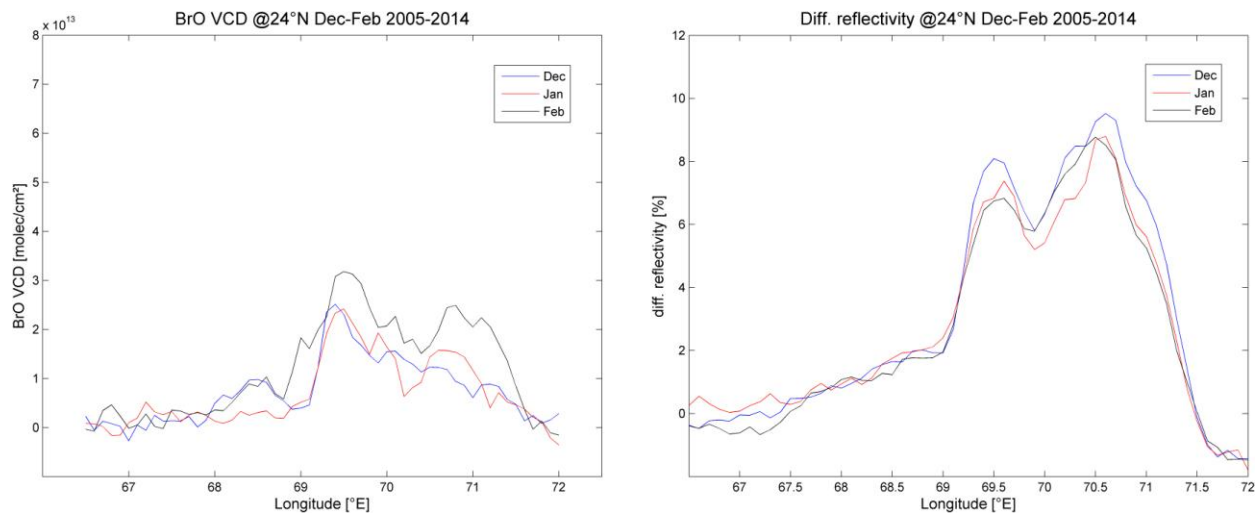


**Figure S5.** Mean BrO VCD (left) and differential reflectivity (right) in longitudinal direction over the Great Rann of Kutch at 24°N latitude during December-February 2005–2014 (color coded in blue - December, red - January and black - February).

### S3 OMI BrO VCDs 2004–2014

This section includes all monthly mean BrO VCD maps for the Rann of Kutch salt marsh to illustrate the annual variations and the seasonal cycle. For further details please also see Section 4 of the main paper.

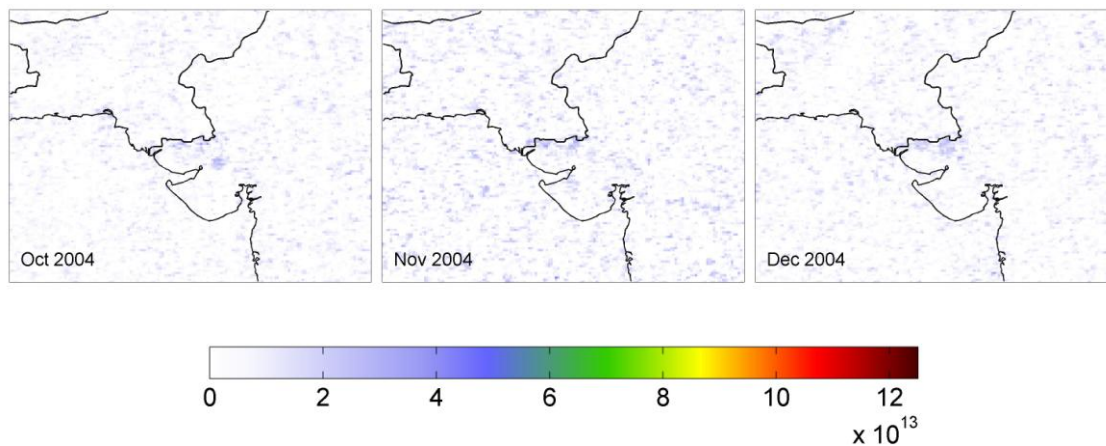


**Figure S6.** Seasonal variation of monthly mean BrO VCD over the Rann of Kutch as seen by OMI during 2004. Please note that OMI data is only available since October 2004.

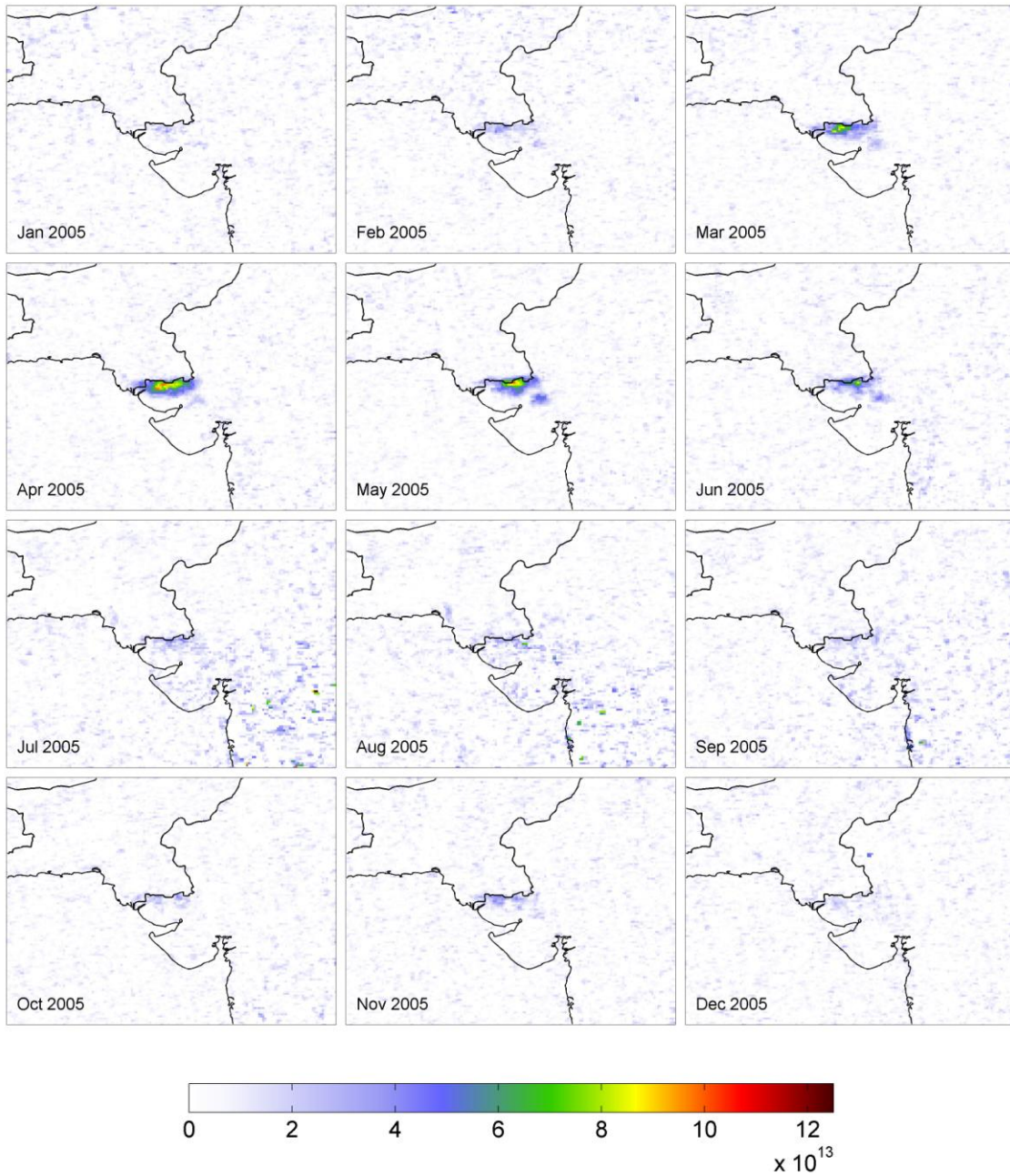


**Figure S7.** Seasonal variation of monthly mean BrO VCD over the Rann of Kutch as seen by OMI during 2005.

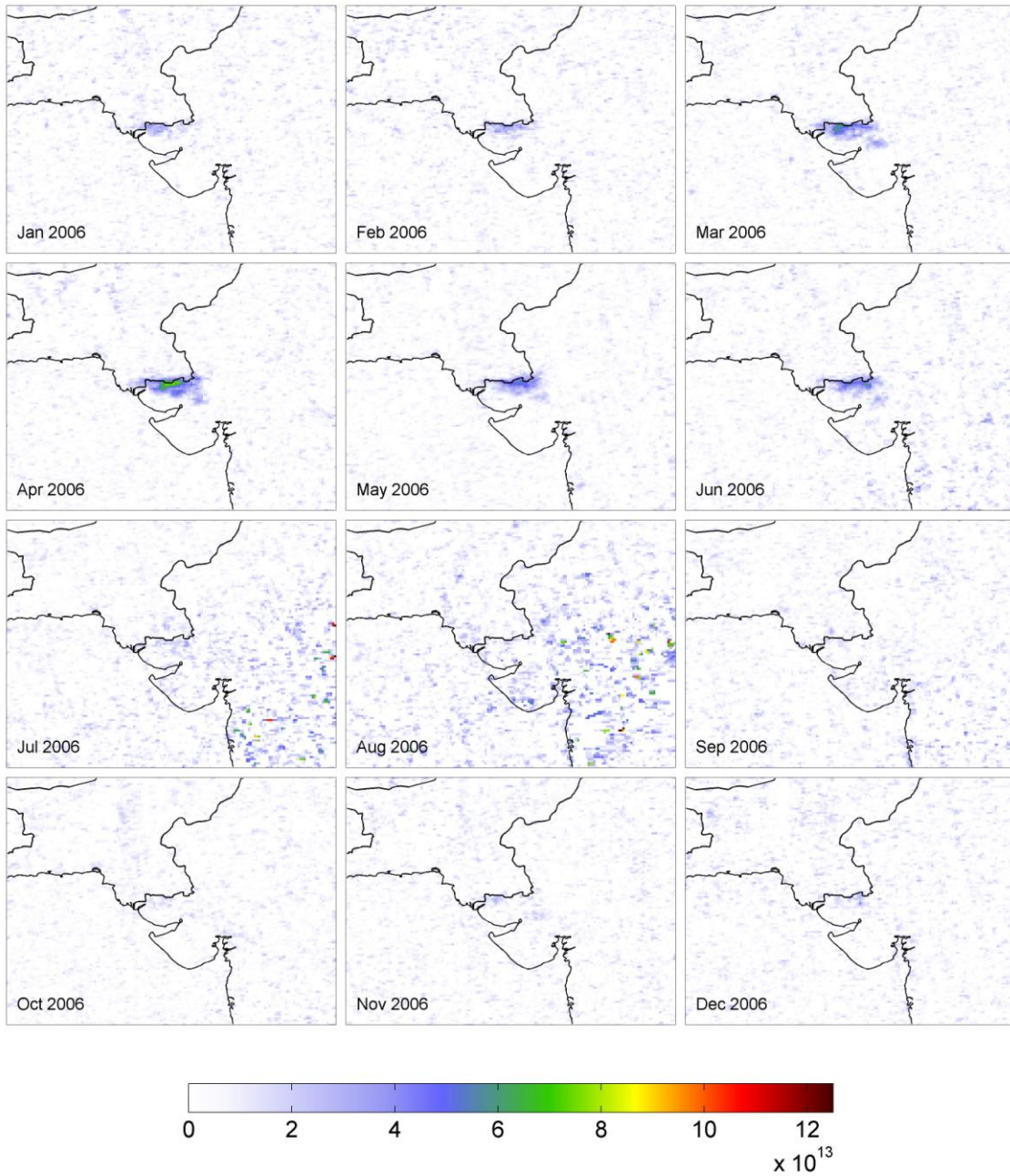


**Figure S8.** Seasonal variation of monthly mean BrO VCD over the Rann of Kutch as seen by OMI during 2006.

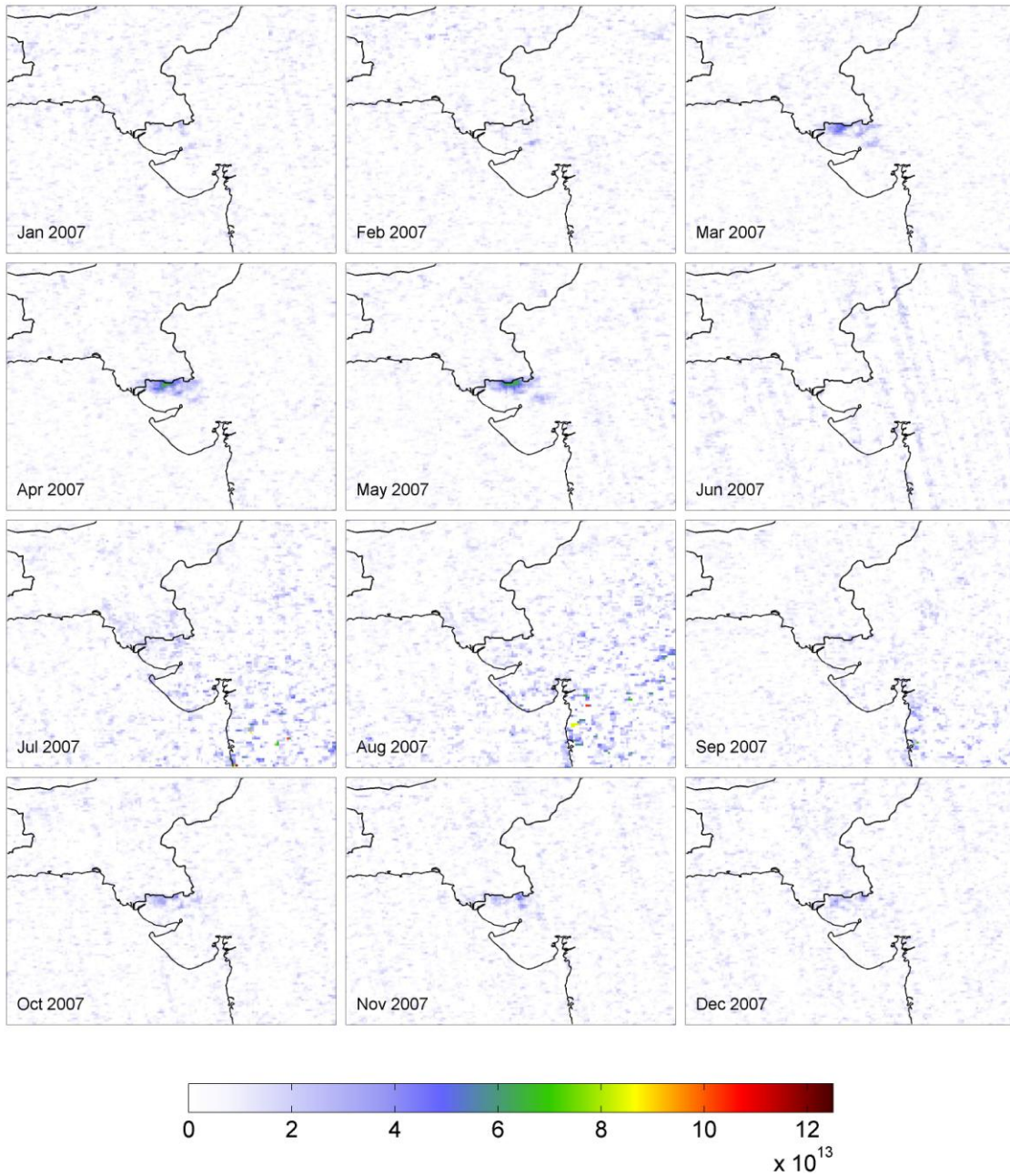


**Figure S9.** Seasonal variation of monthly mean BrO VCD over the Rann of Kutch as seen by OMI during 2007.

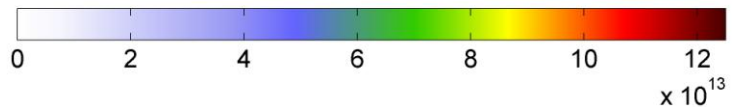
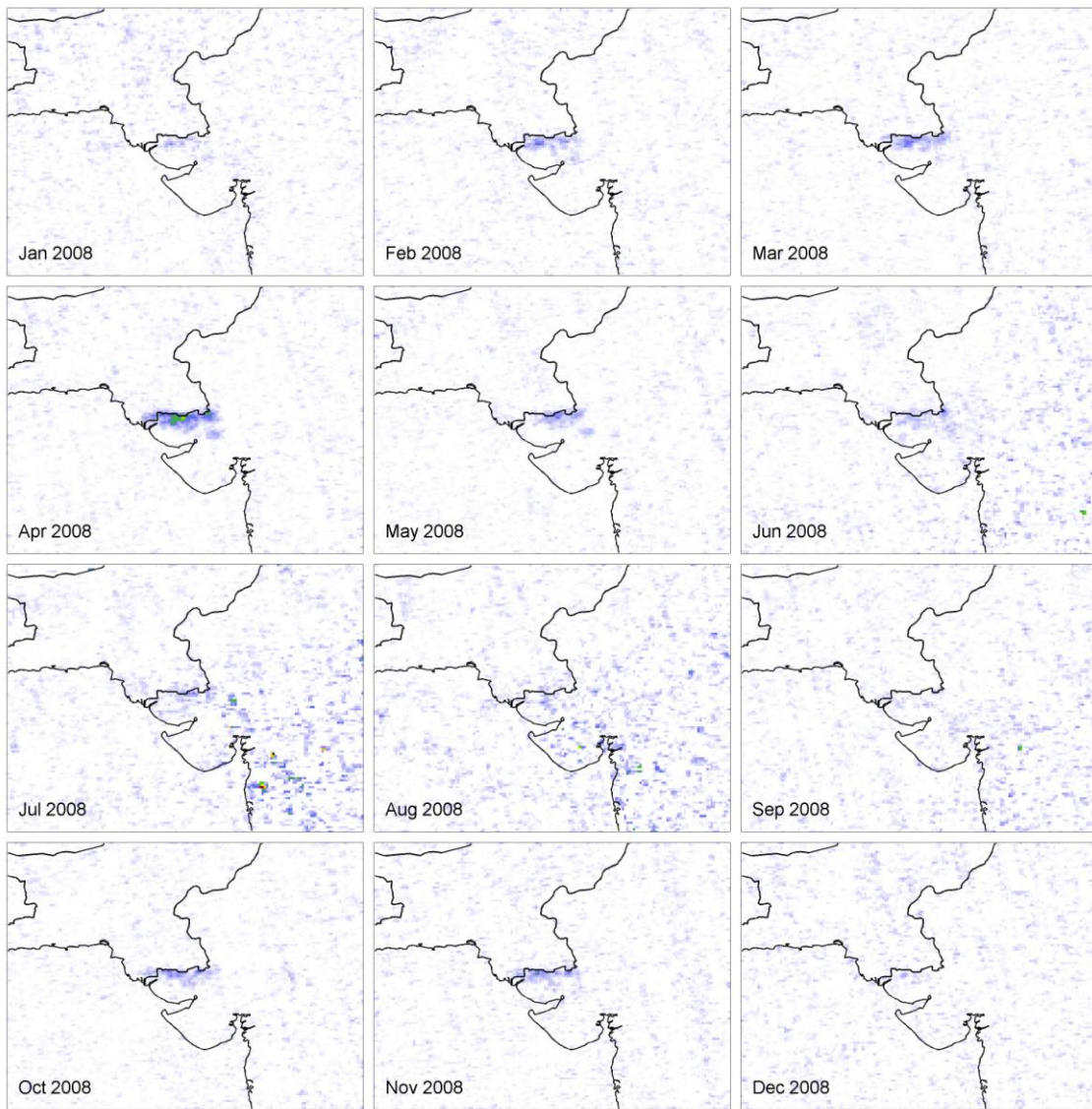


**Figure S10.** Seasonal variation of monthly mean BrO VCD over the Rann of Kutch as seen by OMI during 2008.

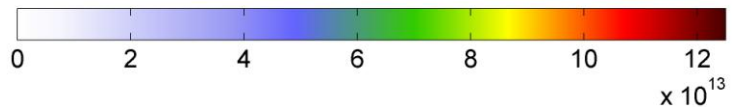
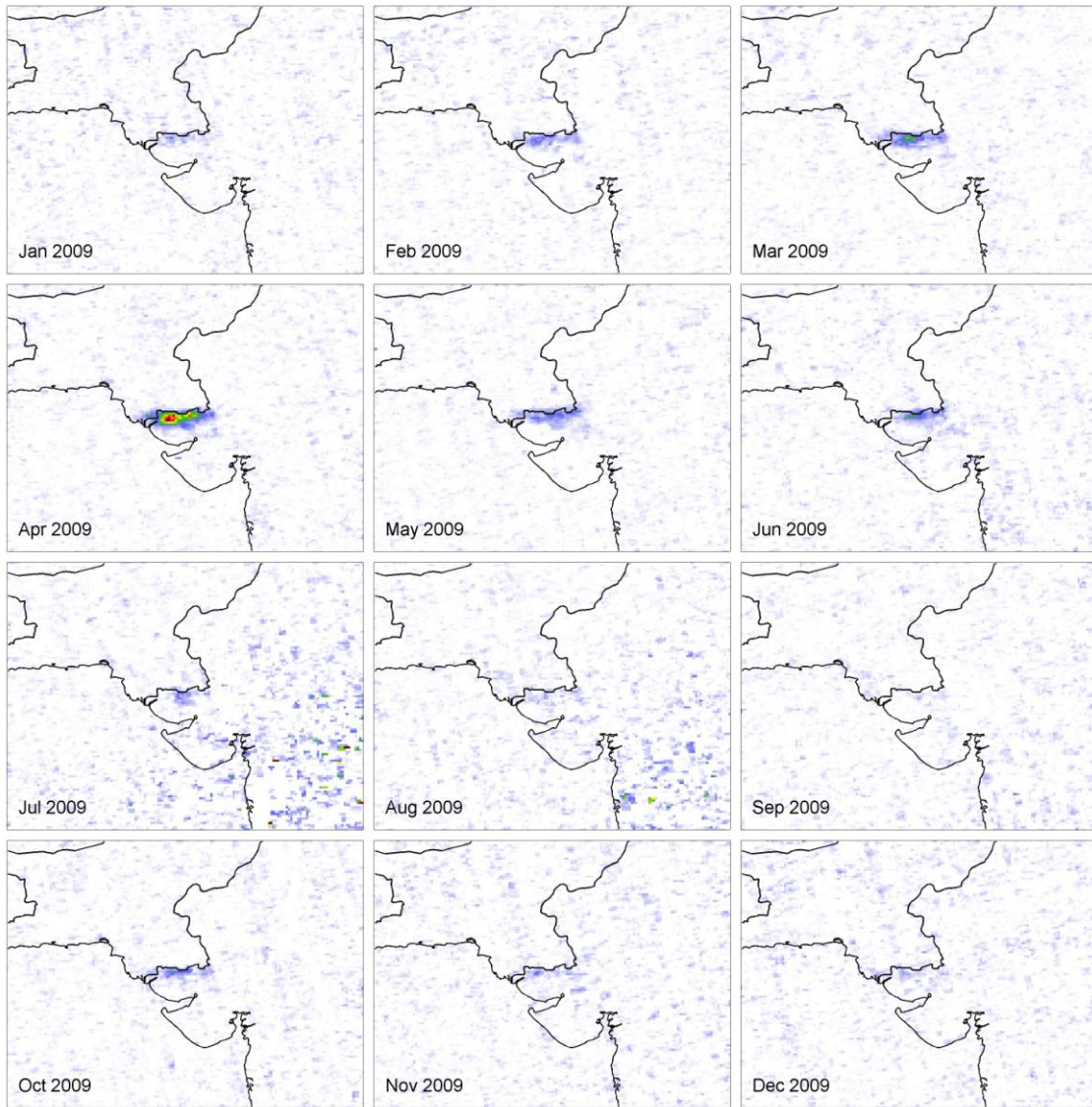


**Figure S11.** Seasonal variation of monthly mean BrO VCD over the Rann of Kutch as seen by OMI during 2009.

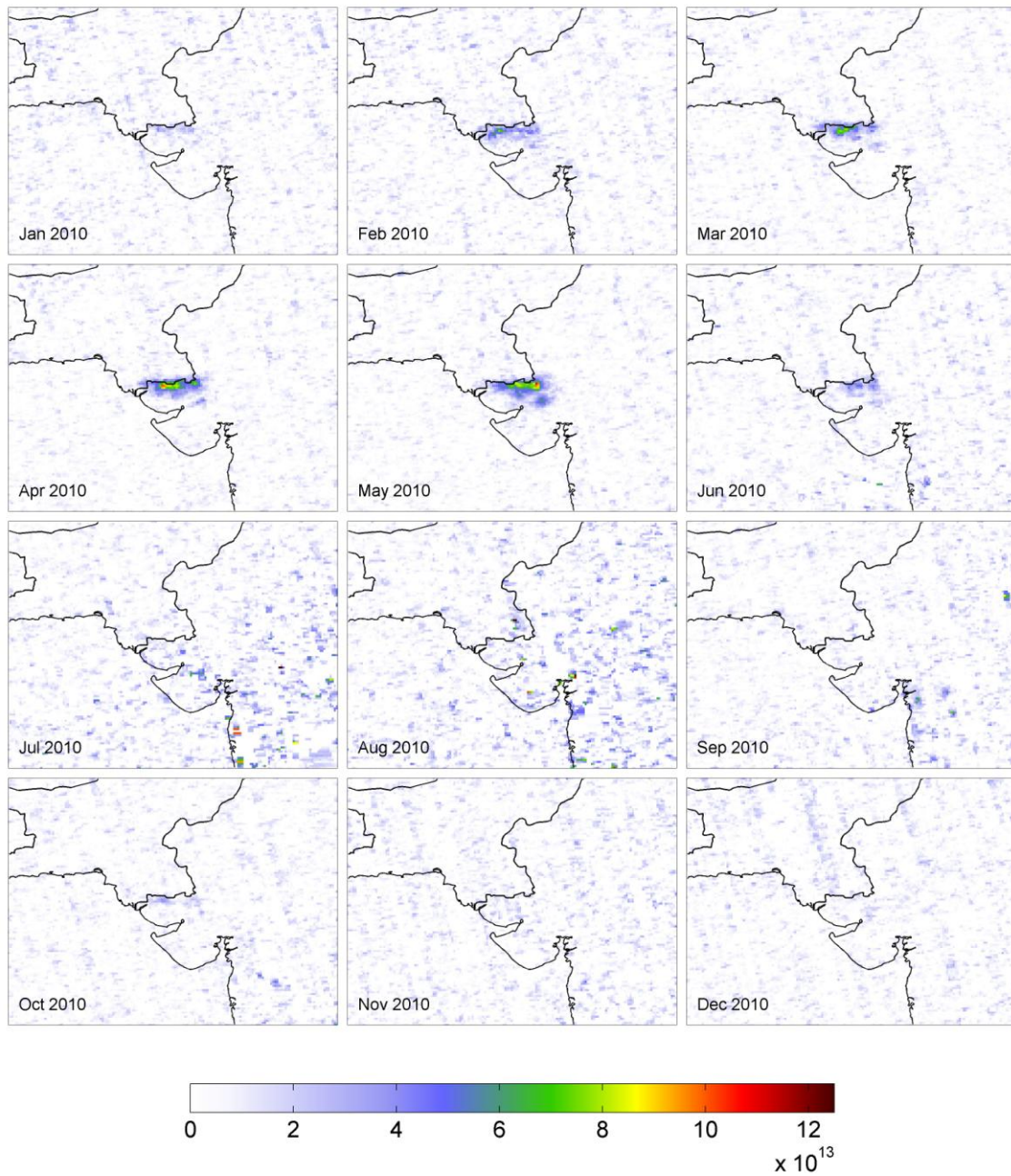


**Figure S12.** Seasonal variation of monthly mean BrO VCD over the Rann of Kutch as seen by OMI during 2010.

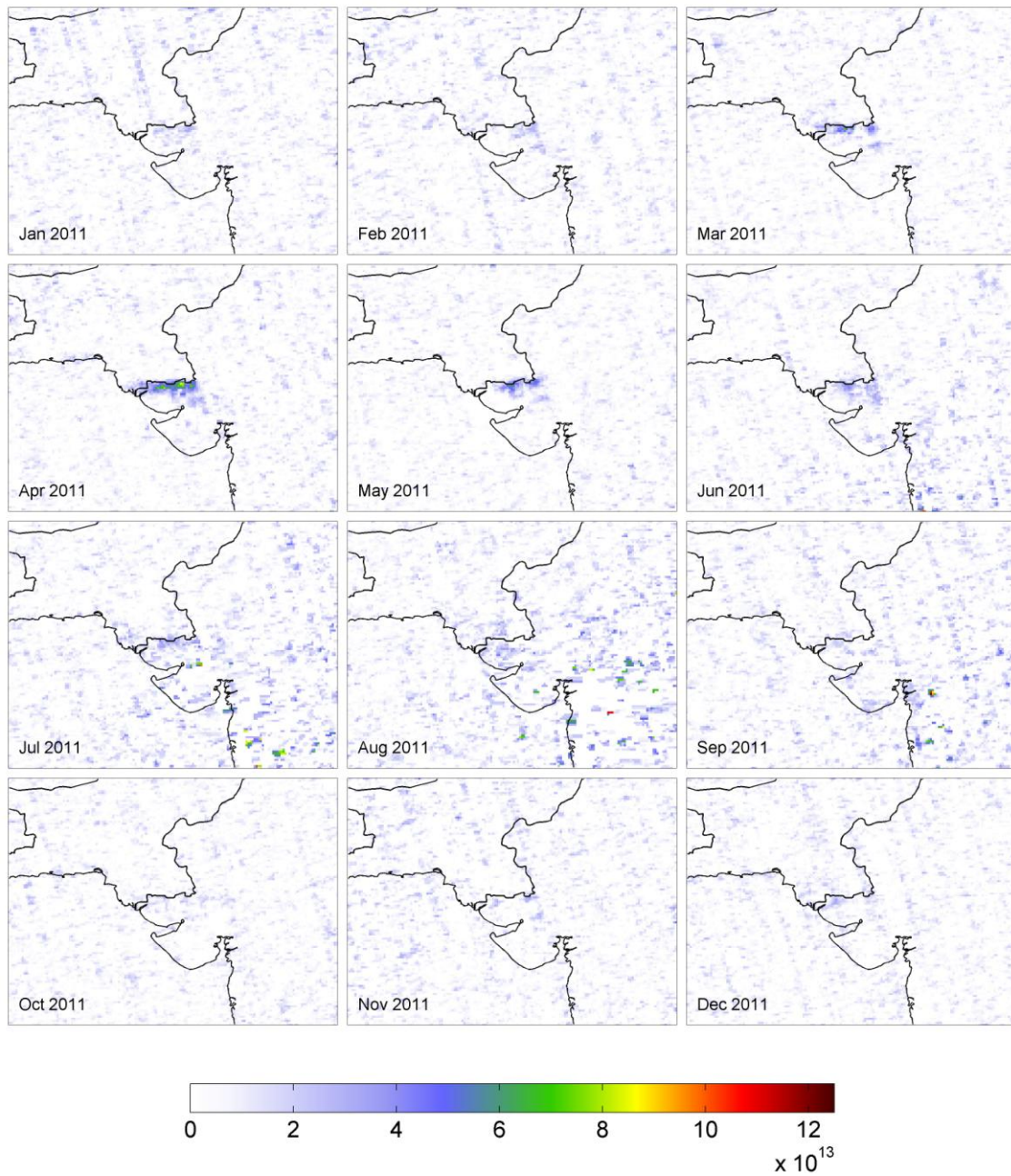


**Figure S13.** Seasonal variation of monthly mean BrO VCD over the Rann of Kutch as seen by OMI during 2011.

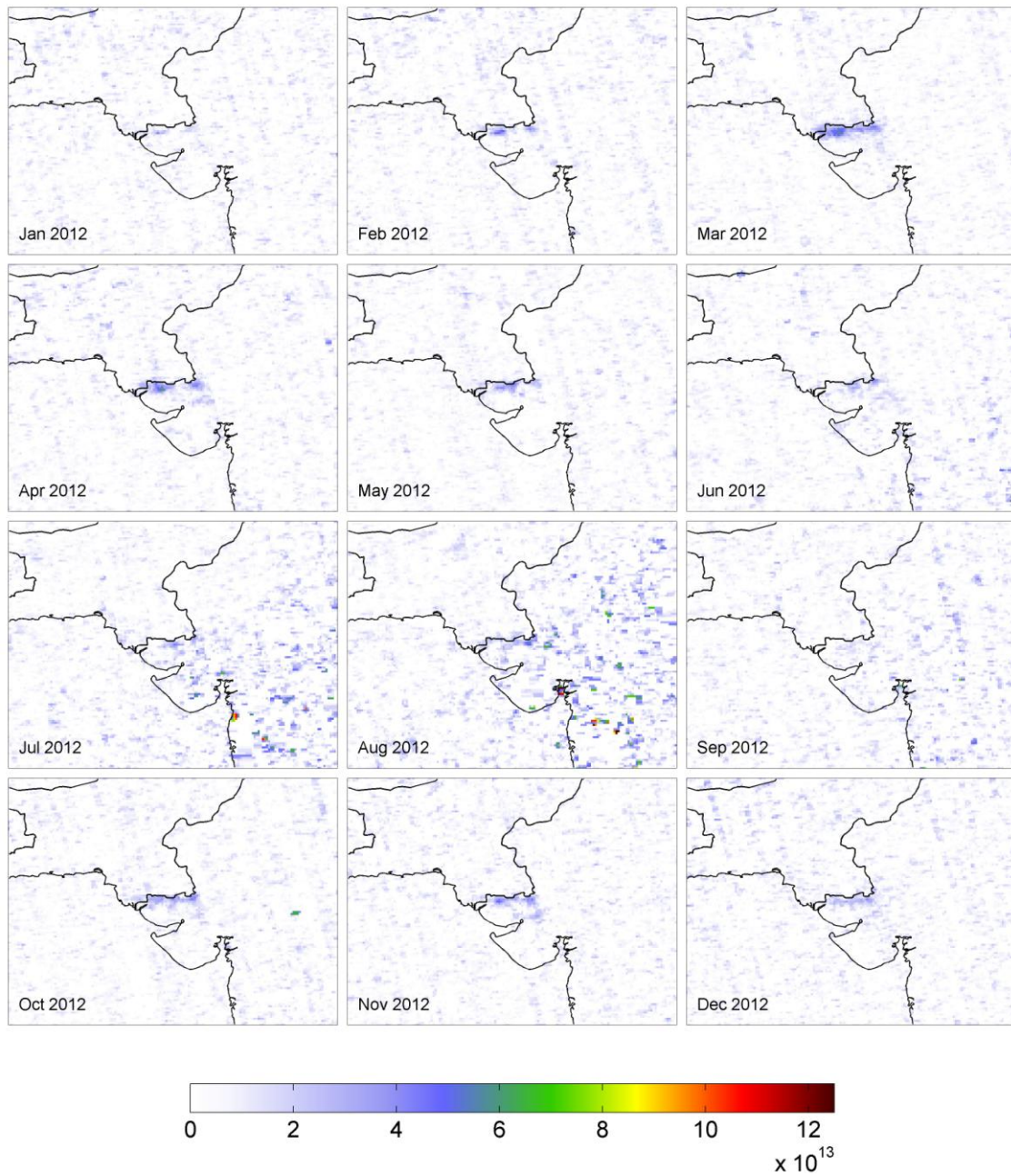


**Figure S14.** Seasonal variation of monthly mean BrO VCD over the Rann of Kutch as seen by OMI during 2012.

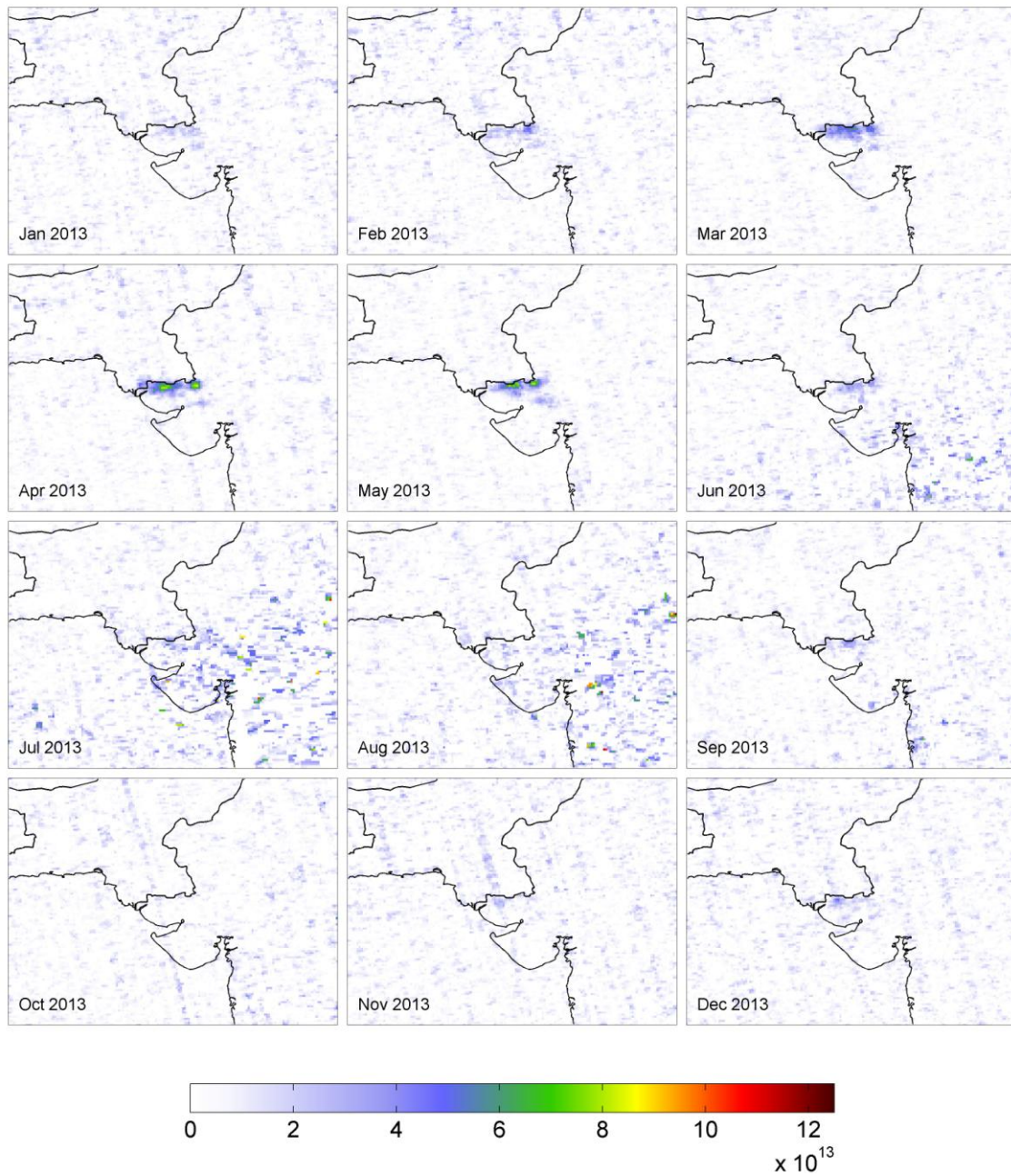


**Figure S15.** Seasonal variation of monthly mean BrO VCD over the Rann of Kutch as seen by OMI during 2013.

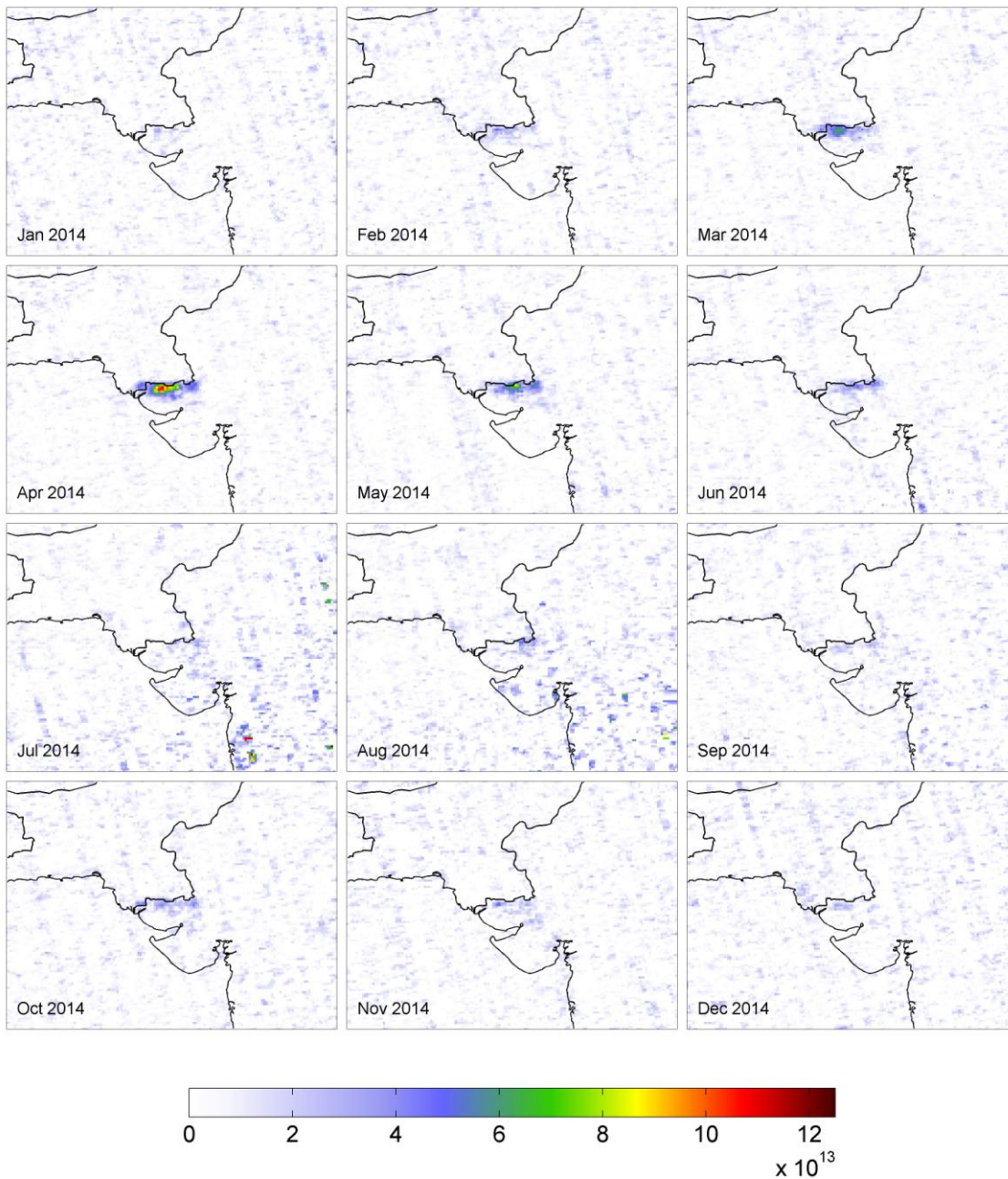


**Figure S16.** Seasonal variation of monthly mean BrO VCD over the Rann of Kutch as seen by OMI during 2014.

#### S4 OMI Reflectivity at 331 nm 2004–2014

This section includes all OMI monthly mean maps of the reflectivity at 331 nm over the Rann of Kutch salt marsh to illustrate the annual variations. For further details please also see Section 4.1 of the main paper.

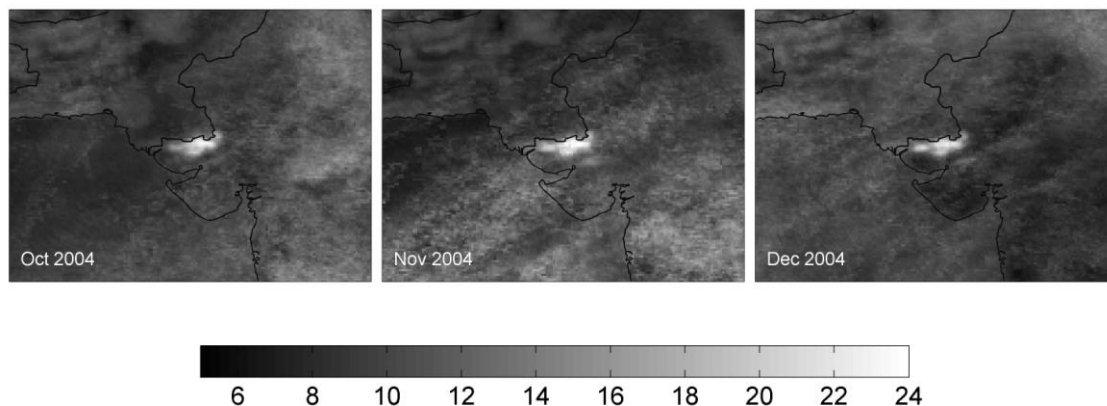


**Figure S17.** Seasonal variation of the monthly mean reflectivity at 331 nm over the Rann of Kutch as seen by OMI during 2004 (same data selection as in Figure S6, i.e. for  $CF < 0.3$ ). Please note that OMI data is only available since October 2004.

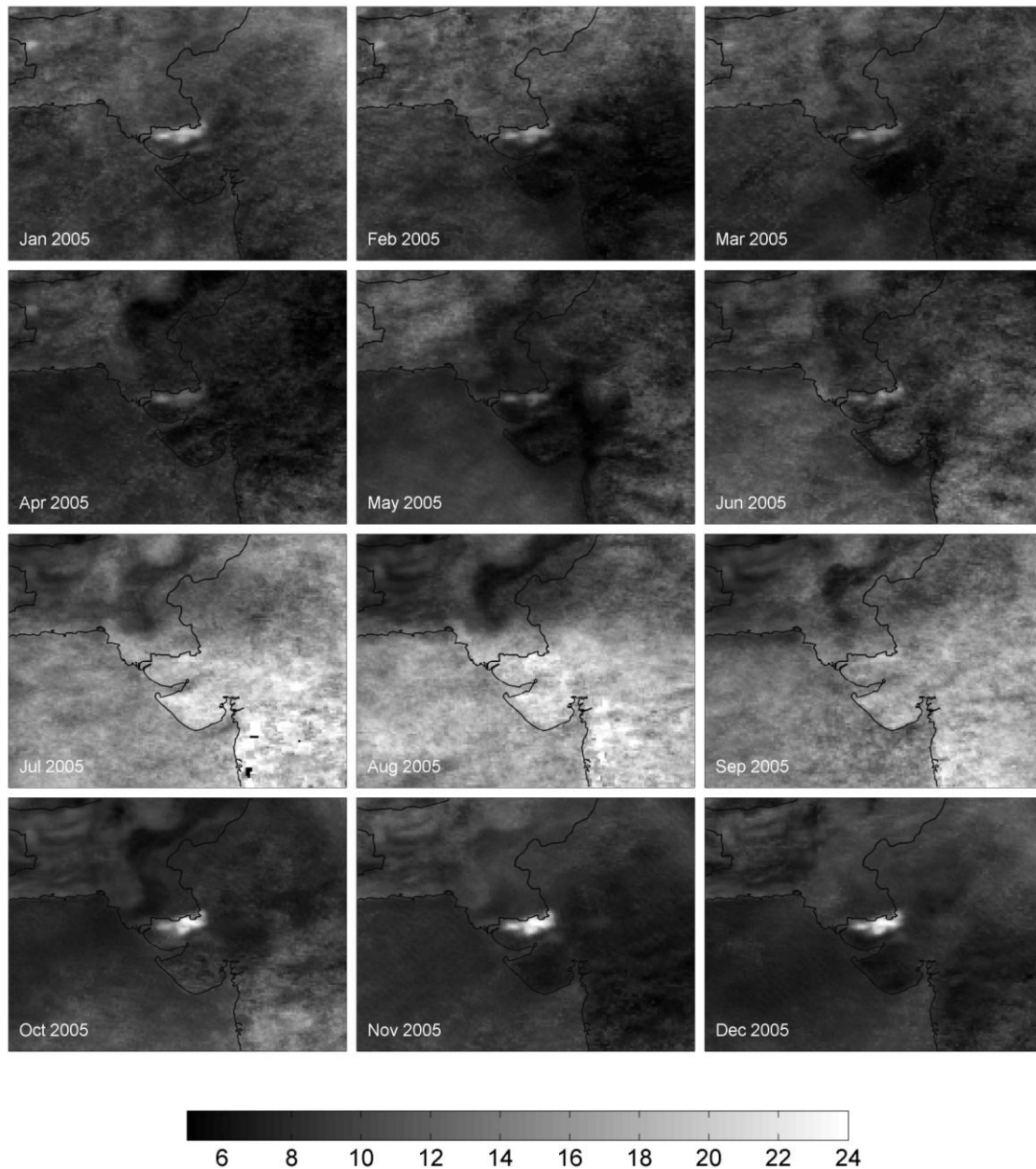


**Figure S18.** Seasonal variation of the monthly mean reflectivity at 331 nm over the Rann of Kutch as seen by OMI during 2005 (same data selection as in Figure S7, i.e. for  $CF < 0.3$ ).

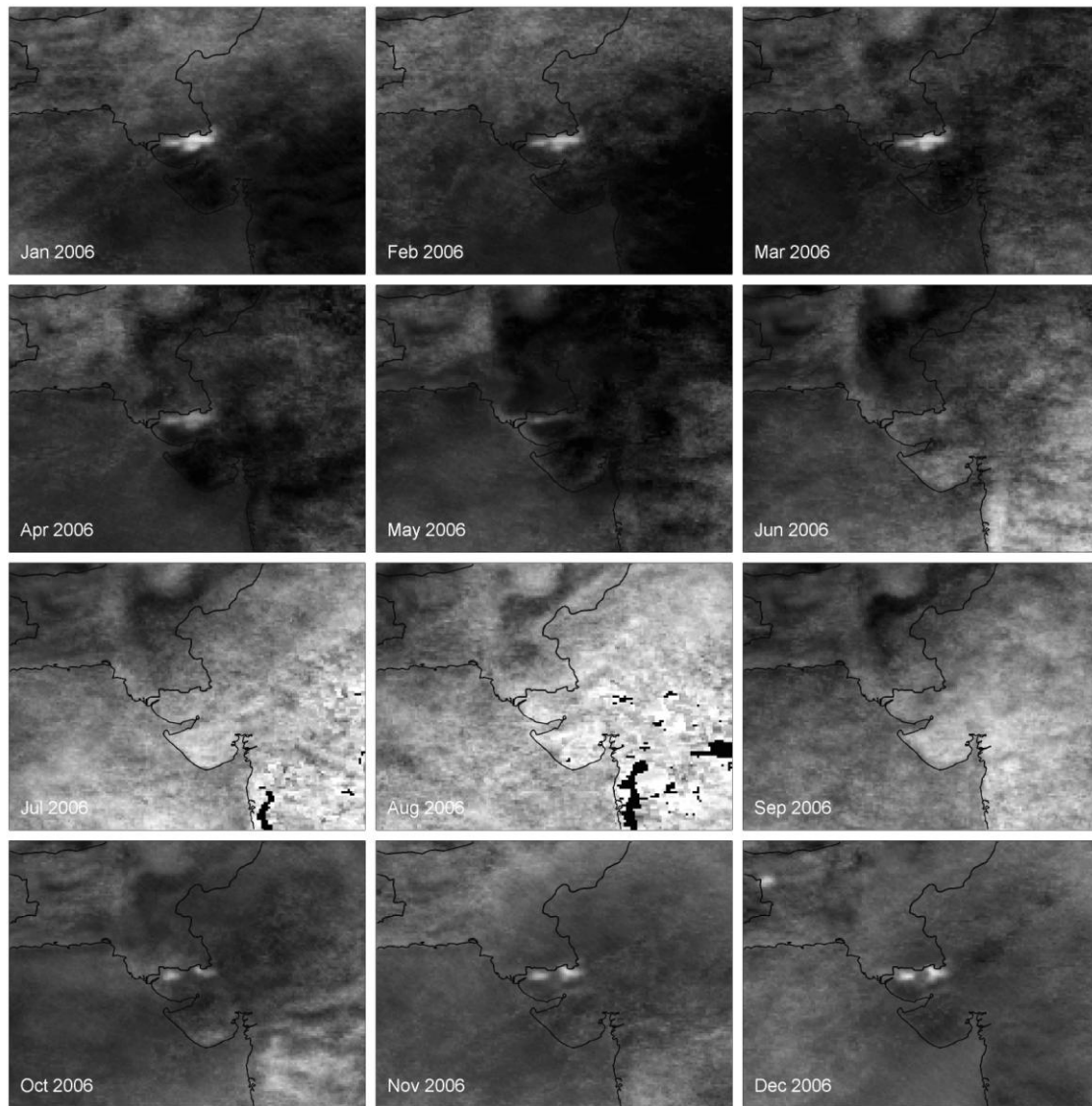


**Figure S19.** Seasonal variation of the monthly mean reflectivity at 331 nm over the Rann of Kutch as seen by OMI during 2006 (same data selection as in Figure S8, i.e. for  $CF < 0.3$ ).

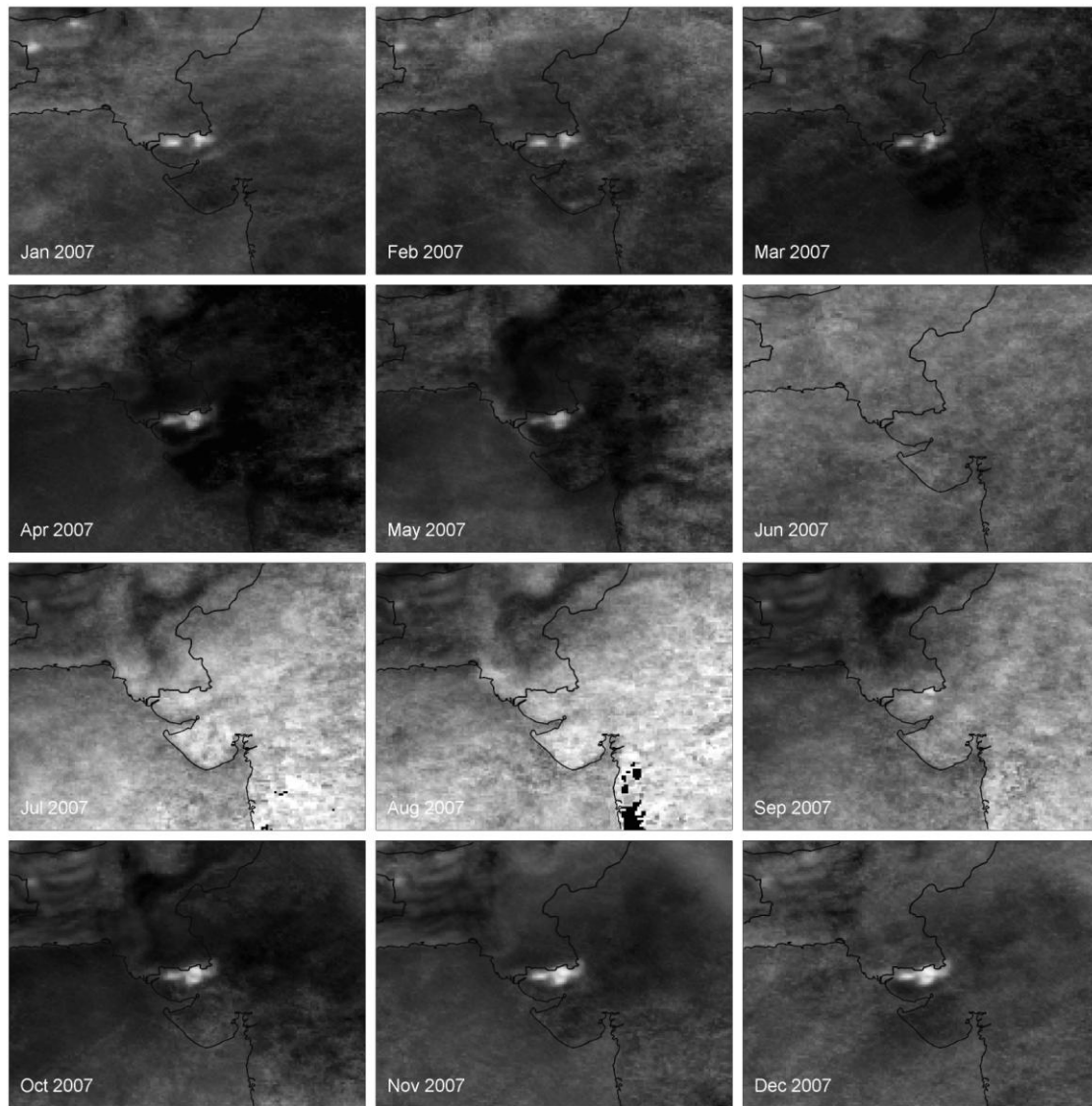


**Figure S20.** Seasonal variation of the monthly mean reflectivity at 331 nm over the Rann of Kutch as seen by OMI during 2007 (same data selection as in Figure S9, i.e. for  $CF < 0.3$ ).

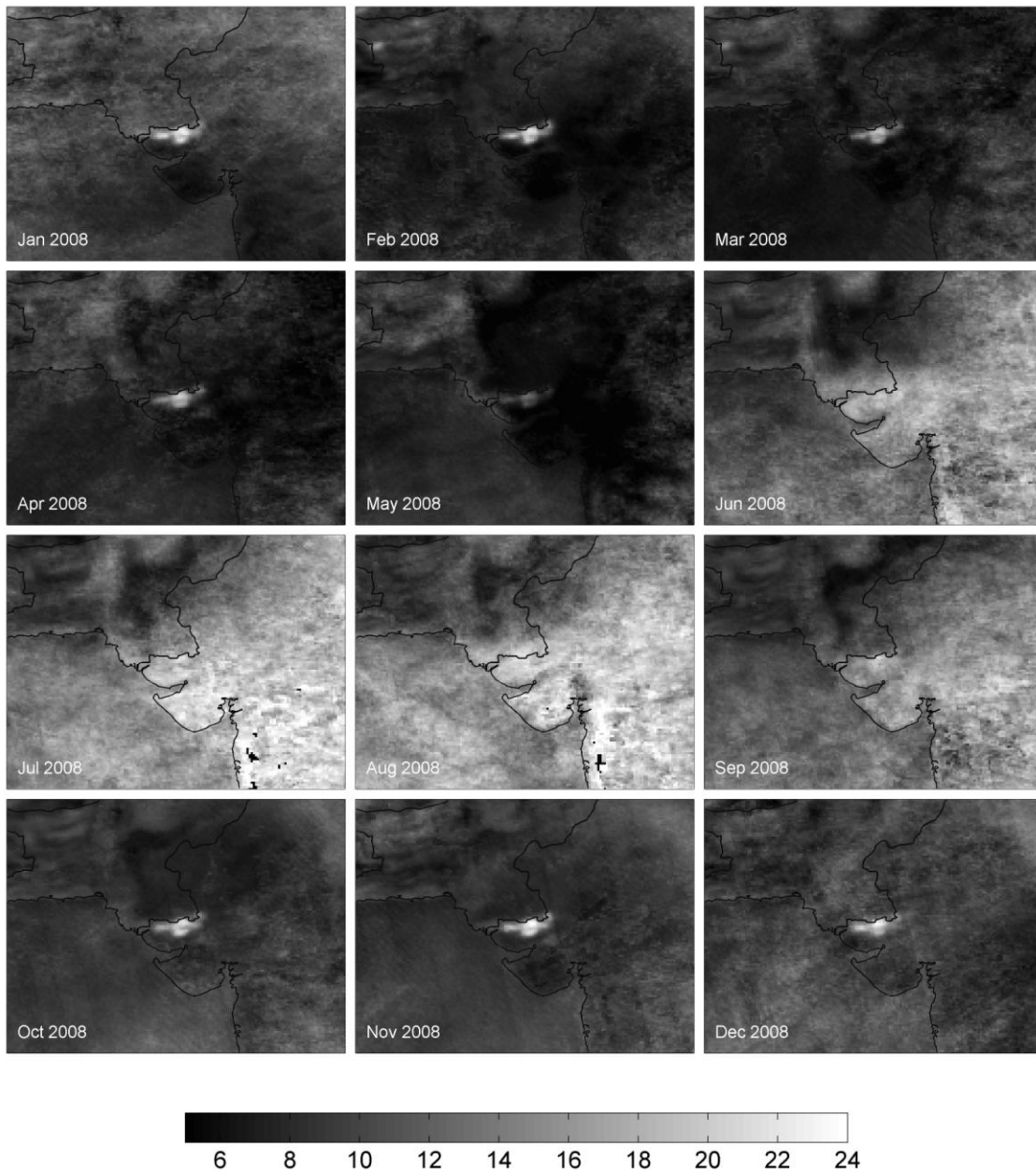


**Figure S21.** Seasonal variation of the monthly mean reflectivity at 331 nm over the Rann of Kutch as seen by OMI during 2008 (same data selection as in Figure S10, i.e. for  $CF < 0.3$ ).

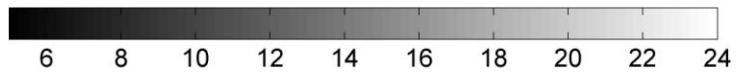
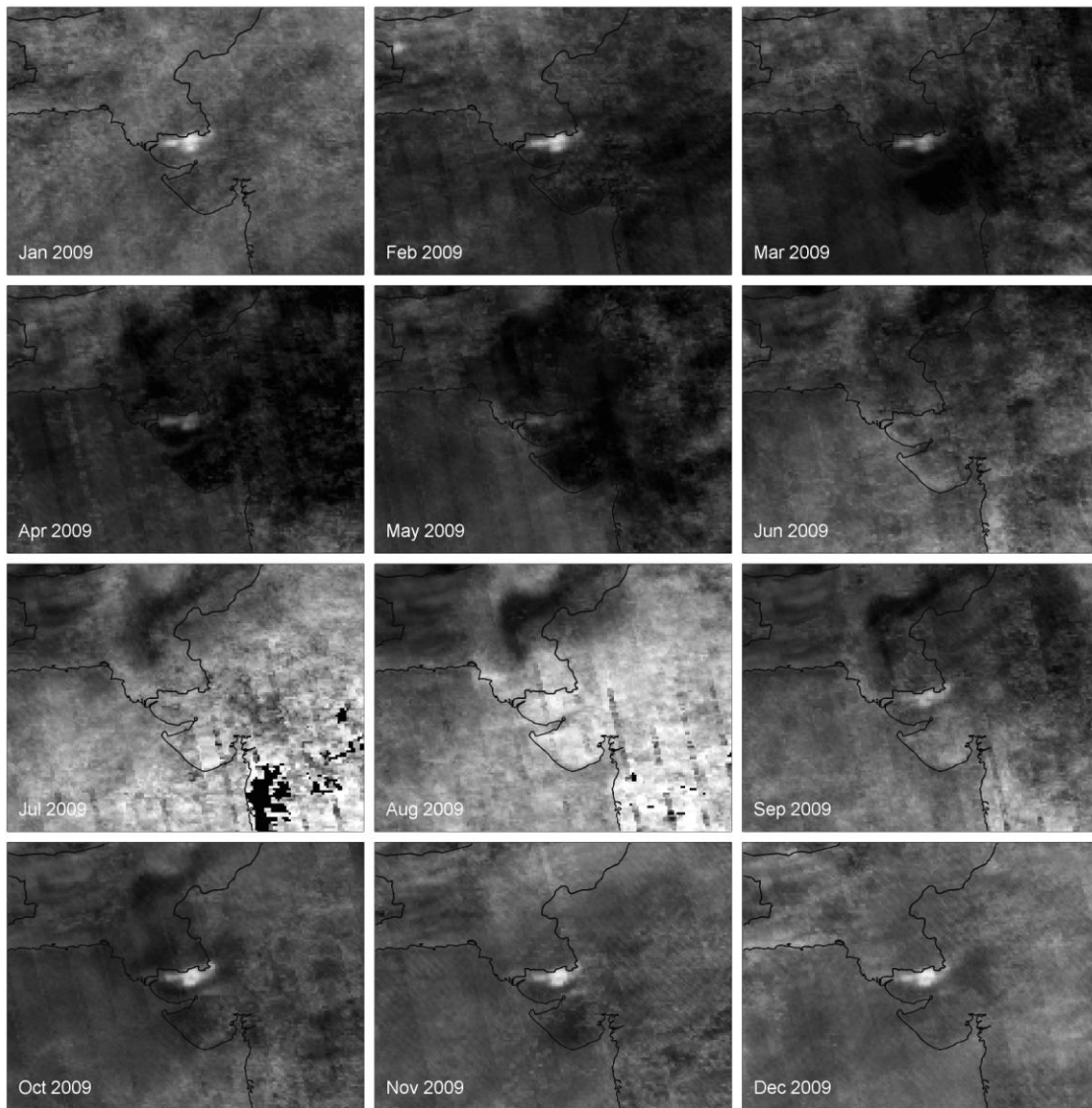


**Figure S22.** Seasonal variation of the monthly mean reflectivity at 331 nm over the Rann of Kutch as seen by OMI during 2009 (same data selection as in Figure S11, i.e. for  $CF < 0.3$ ).

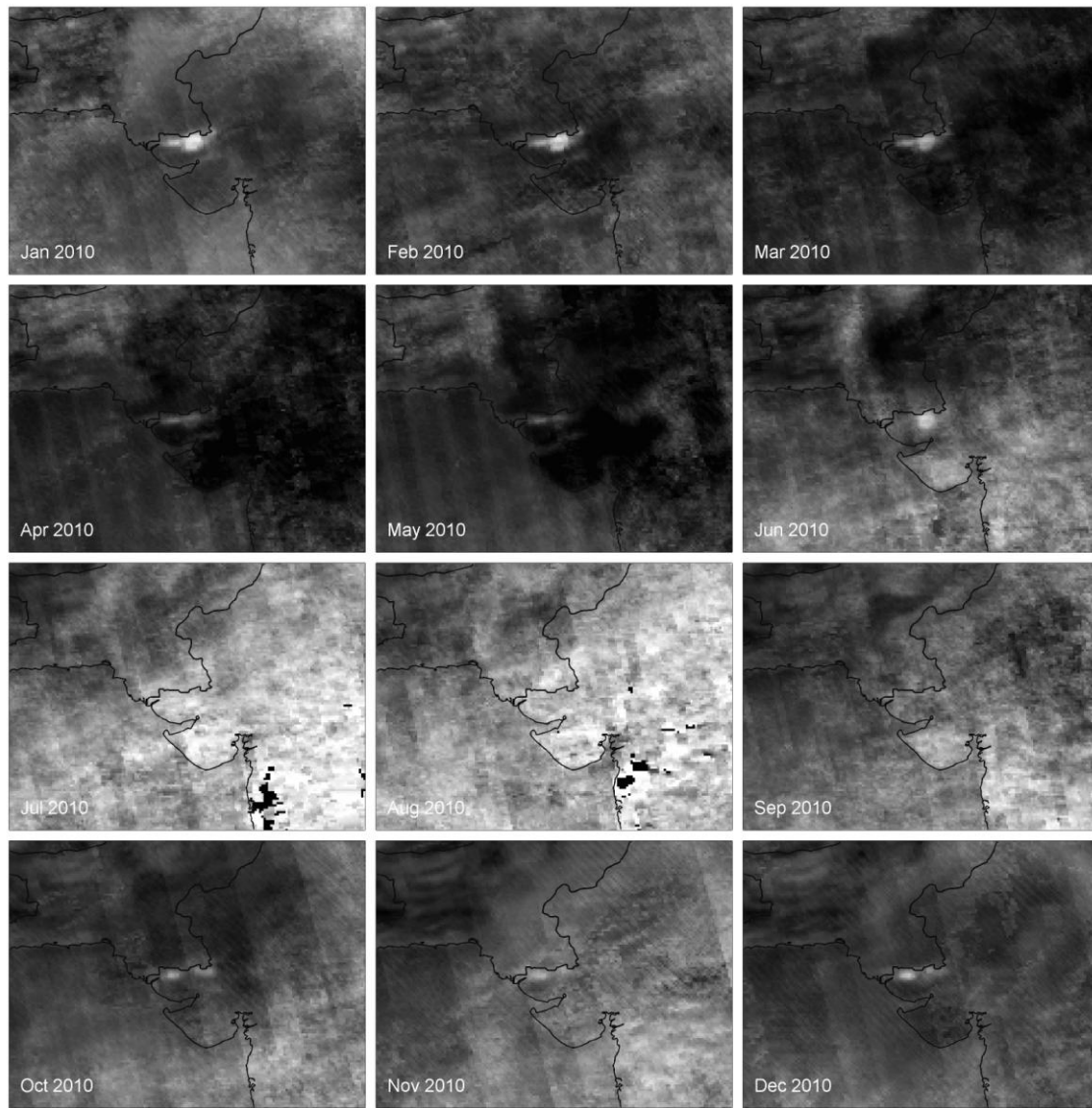


**Figure S23.** Seasonal variation of the monthly mean reflectivity at 331 nm over the Rann of Kutch as seen by OMI during 2010 (same data selection as in Figure S12, i.e. for  $CF < 0.3$ ).

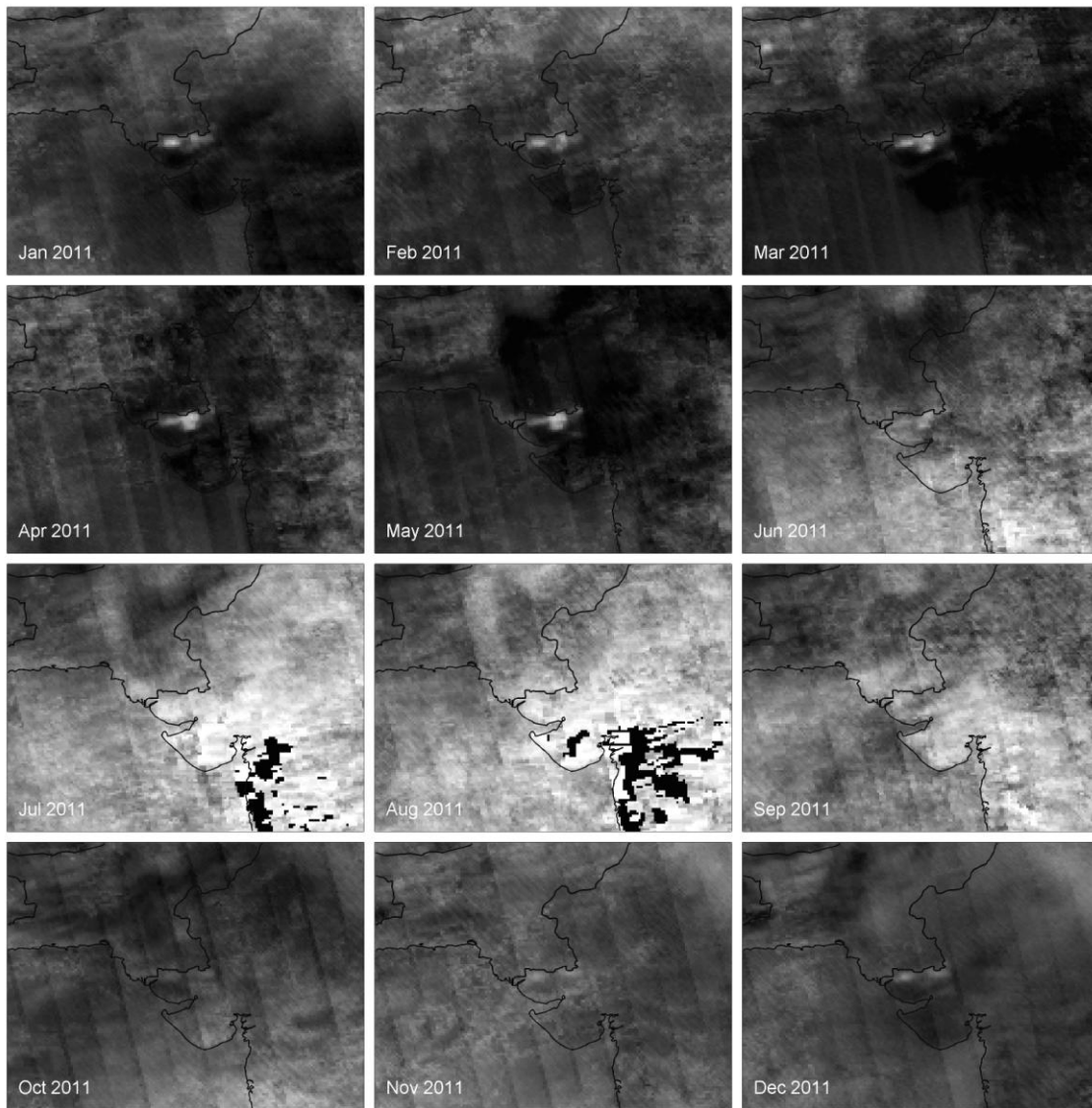


**Figure S24.** Seasonal variation of the monthly mean reflectivity at 331 nm over the Rann of Kutch as seen by OMI during 2011 (same data selection as in Figure S13, i.e. for  $CF < 0.3$ ).

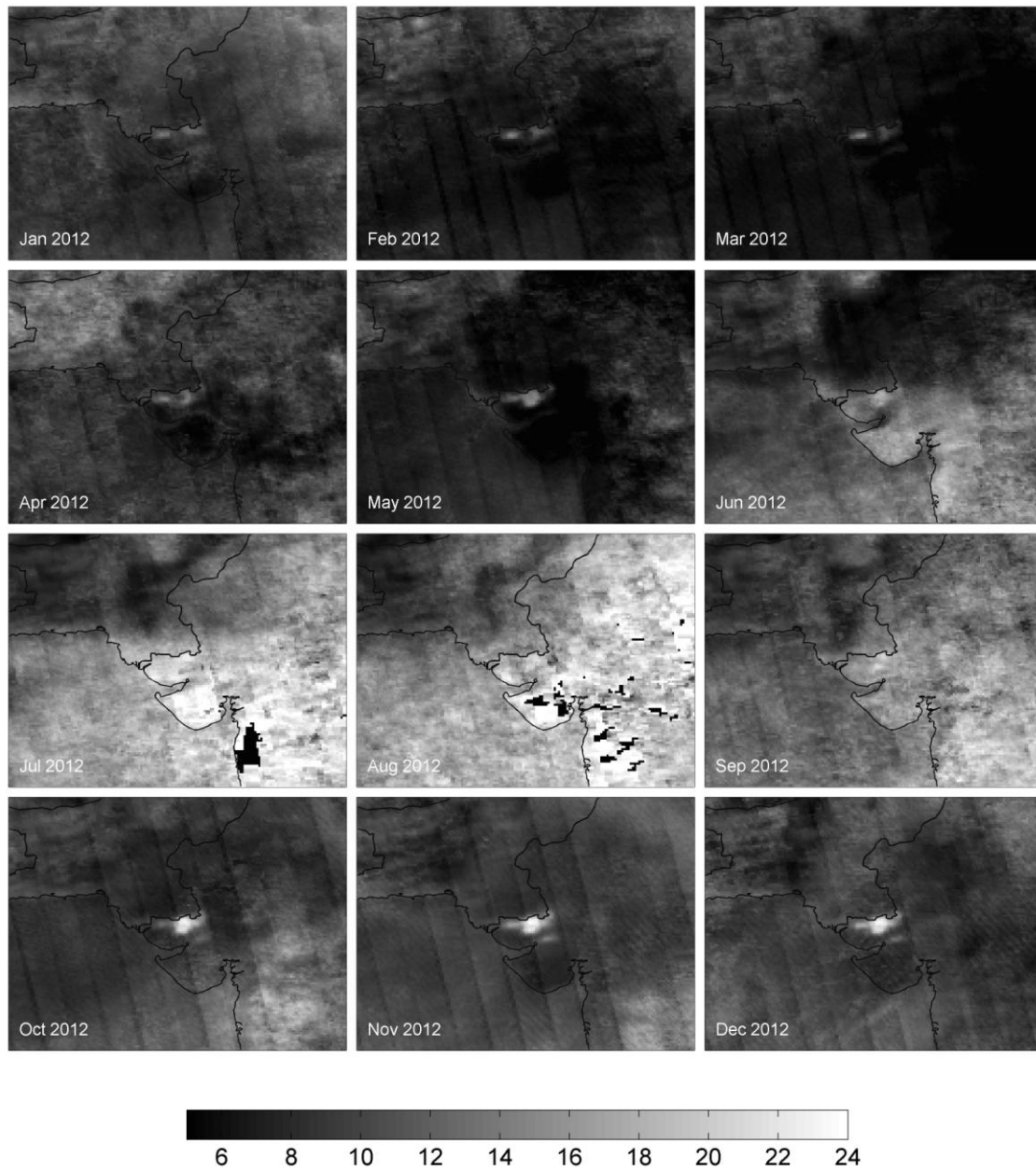


**Figure S25.** Seasonal variation of the monthly mean reflectivity at 331 nm over the Rann of Kutch as seen by OMI during 2012 (same data selection as in Figure S14, i.e. for  $CF < 0.3$ ).

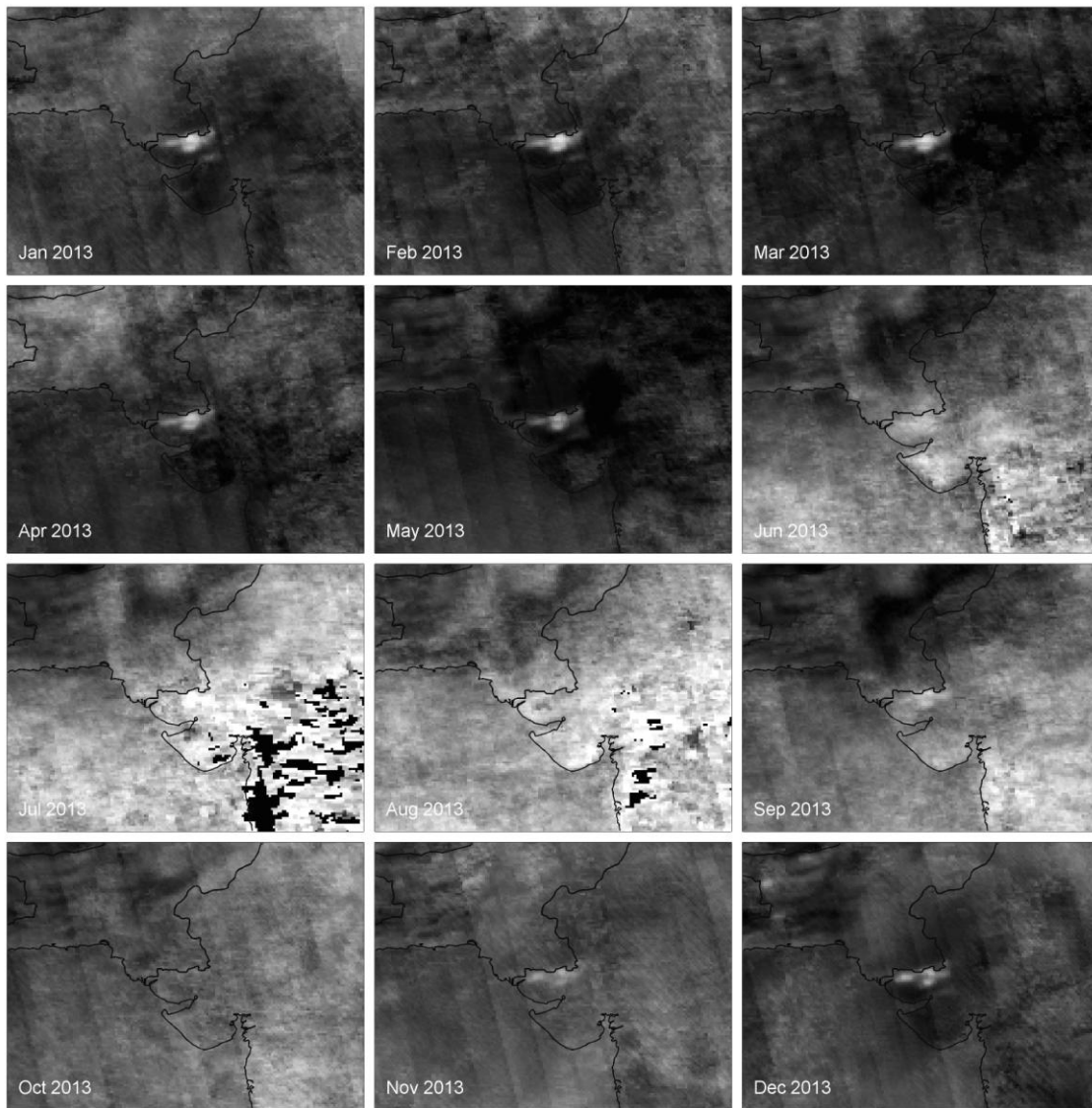


**Figure S26.** Seasonal variation of the monthly mean reflectivity at 331 nm over the Rann of Kutch as seen by OMI during 2013 (same data selection as in Figure S15, i.e. for  $CF < 0.3$ ).

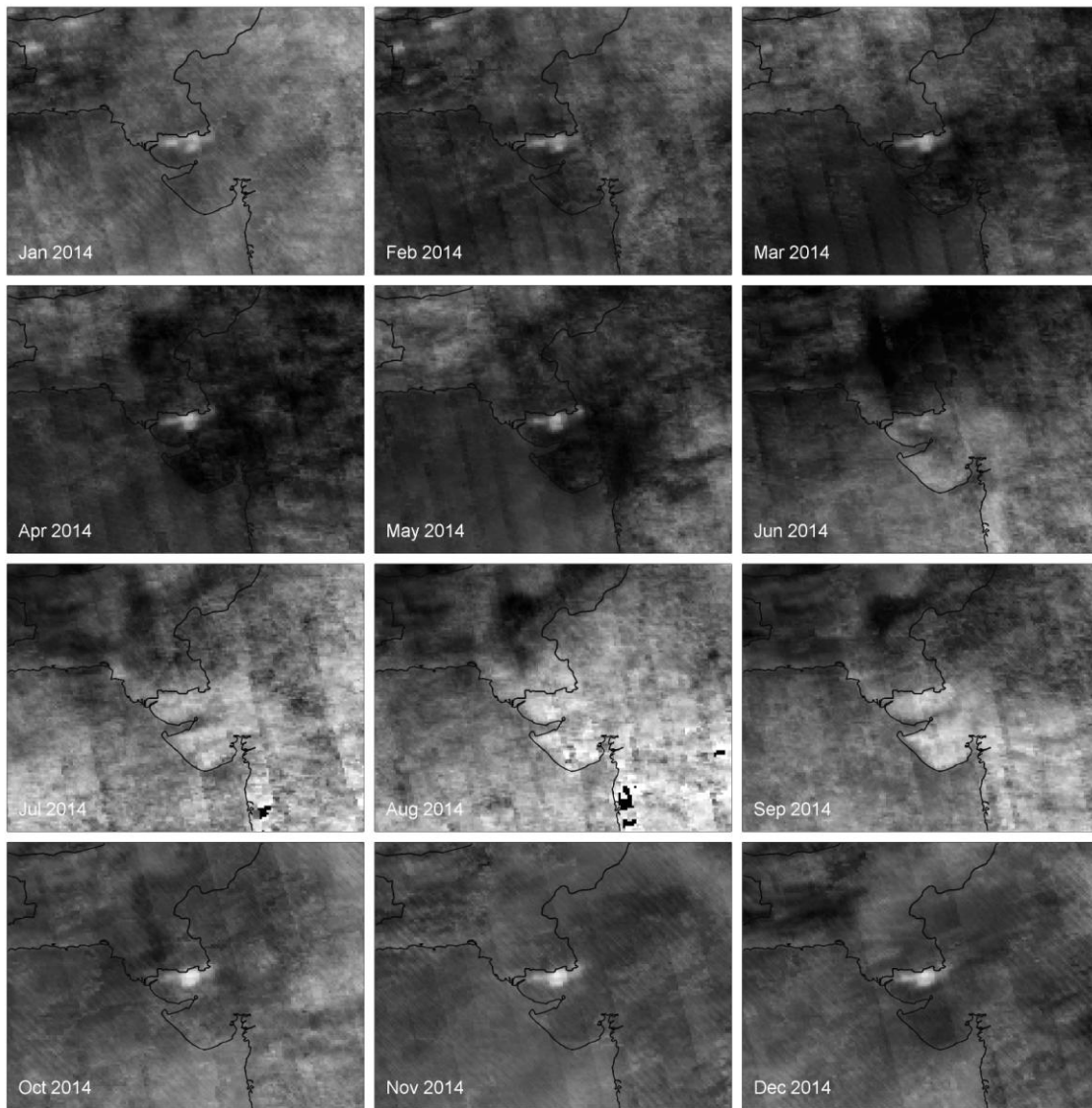


**Figure S27.** Seasonal variation of the monthly mean reflectivity at 331 nm over the Rann of Kutch as seen by OMI during 2014 (same data selection as in Figure S16, i.e. for  $CF < 0.3$ ).